CO dispersion from a coal fire in a mine entry

J.C. Edwards, R.A. Franks, G.F. Friel & L. Yuan
National Institute for Occupational Safety and Health, Pittsburgh Research Laboratory, Pittsburgh, PA, USA

ABSTRACT: Five mine fire experiments were conducted in a 2.08 m high and 2.90 m wide, ventilated mine entry in the National Institute for Occupational Safety and Health (NIOSH)'s Safety Research Coal Mine (SRCM) to determine the effect of the dispersion of carbon monoxide (CO) on mine fire detection. CO measurements were made at distances from 7.6 m to 45.2 m downwind from the fire with diffusion mode CO sensors positioned near the roof. For small intensity fires, less than 30 kW heat release rate, generated by 14 kg coal in a 0.61 m square tray, it was determined that air flow and sensor spacing were significant for fire detection at the 10 ppm CO alarm level. Within 15.0 m downwind distance from the fire, 10 ppm CO alarm values occurred for volumetric air flows less than 11.5 m^3/s. However, the 10 ppm CO alarm value did not occur 30.0 m downwind from the fire for air quantities greater than 6.2 m^3/s due to dilutive mixing of the CO in the air stream. The criterion that the mine fire alarms occur within 15 min of the onset of flaming combustion could not be consistently met with the 10 ppm CO alarm. This suggests the use of lower CO alarm values, or reduced CO sensor spacings for mine fire protection. It is demonstrated how computational fluid dynamics (CFD) can be used to model the CO dispersion downwind from the fire in support of a plan to optimize sensor spacings.

Disclaimer: The findings and conclusions in this report are those of the authors and do not necessarily represent the views of the National Institute for Occupational Safety and Health.

1 INTRODUCTION

The deployment of carbon monoxide (CO) sensors in a mine entry to achieve early and reliable fire detection is important for miner safety. The Code of Federal Regulations (2004) specifies CO sensor spacing distances for a belt air-course. The fire source location for a fire in a belt air-course typically occurs on the entry floor, or near the entry half-height associated with the conveyor belt structure. Fires could occur due to frictional heating at the belt drive and along the belt. Coal which has accumulated on a belt drive can be heated by roller slippage. Another possible fire source is the ignition of spilled coal on the floor from cutting and welding activity. Previous research (Litton, et al., 1991) has established that approximately 15 min (average time for 15 experiments was 14.3 min with a standard deviation of 7.3 min) after a smoldering coal fire evolves to the flaming stage, a conveyor belt in contact with the fire can be ignited. Early and reliable fire detection is important within this time frame. When a plume of combustion products rises towards the mine roof due to the thermally induced density differences between the hot products-of-combustion (POC) and the ambient air, the POC will also be convected with the bulk air flow downwind from the fire source. The POC will be dispersed by the dilutive mixing with the fresh air over the entry cross-section downwind from the source fire. This dispersion process is enhanced by the thermal equilibration of the POC with the ambient air. It is important to know the expected distribution of CO near the mine roof along the entry in the smoldering and flaming coal fire stage to provide guidance for sensor site location, and the effect of volumetric air flow upon the CO concentration. The objective of this research is to analyze experimentally and computationally the dispersion of CO from small coal fires in a mine entry and determine the sensitivity of CO concentration to ventilation and sensor site location.

2 EXPERIMENTAL CONFIGURATION

The experimental location selected for the fire experiments to determine the effect of air flow and sensor spacing upon fire detection was an entry in NIOSH's SRCM at the Pittsburgh Research Laboratory (PRL). The entry height and width at the location of the fire pan were 1.96 m and 2.79 m, respectively. Since in a mine environment the source fire could occur on a belt drive at entry mid-height, the experiments included both floor and mid-height fire source locations. Coal was selected as the fire fuel source. Five small coal fire experiments were conducted. The CO concentration was measured with diffusion mode Conspec Controls Inc CO monitors near the roof at locations 7.6, 15.0,

30.0, and 45.2 m downwind from the fire pan. (Reference to a specific product is for informational purposes and does not imply endorsement by NIOSH.) At the 7.6 and 15.0 m locations two CO sensors each were located at equally spaced intervals across the entry near the roof. At the 30.0 and 45.2 m stations a single CO sensor was positioned at the entry center near the roof. Calibration of the CO monitors was conducted before each experiment with hydrocarbon free air and 25 ppm CO in air. The entry average height and width were 2.08 m and 2.90 m. The entry associated hydraulic diameter was 2.42 m. Table 1 lists the fire source location and entry air flow for each experiment. Sensor data was collected every 2 seconds with a mine monitoring system. For experiment nos. 1–3 the fire pan was positioned on the mine entry floor, and for experiment nos. 4 and 5 the fire pan was positioned on a set of blocks 0.89 m above the floor, which is approximately half the 1.96 m entry height at the fire zone. For each experiment about 14 kg of run-of-the-mine Pittsburgh Seam coal contained in a 0.61 m square tray was heated by embedded electrical strip heaters. A small quantity, about 0.5 kg, of pulverized Pittsburgh Seam coal was added to the coal. Heating of pulverized coal provided an early source of CO. Electrical power was supplied to the strip heaters over a 30 min period with an increase from 1.7 to 2.8 kW. The slow increase in heating was to produce incipient CO emissions at the lowest power source available, and to simulate the slow heating to be expected from a heated element, such as at a belt drive or along the belt. The linear air flow measurements were made with a Solomat Neotronics hot wire anemometer for experiment nos. 1–4. An average linear air flow was determined from a five point average measurement over the entry cross-section. The Solomat was not temperature compensated. A correction to the Solomat measured air flow was made based upon a calibration of the Solomat with an Edra 6 Air flow Developments Ltd vane anemometer over a temperature range from 25 to 73 deg F. For the four temperature evaluations a linear fit was made which had an R-square value, coefficient of determination, equal to 0.9973. The corrected air flow values at the fire pan are listed in Table 1. The volumetric air flow refers to the entry cross-section at the fire pan. For experiment no. 5 an ultrasonic flow monitor from El-Equip Inc was used. The ultrasonic flow monitor measures the average air flow along a diagonal between the entry's opposing ribs.

3 RESULTS

For all five experiments the CO measurements at the 7.6 and 15.0 m stations indicated the CO dispersion was uniform over the midsection near the roof. Consequently, the CO concentration at these two locations was represented as an average. Experiment nos. 2 and 5 provide a comparison of the time dependent CO concentration at the sensor stations with a fire on the mine entry floor and at entry mid-height. These two experiments are representative of the two experimental configurations for source fire location. Figures 1 and 2 show the measured CO concentration at each station for experiment nos. 2 and 5, respectively. For experiment no. 2 the heat source was increased from 1.7 kW to 2.8 kW over the time period 9:32 to 10:02. For experiment no. 5 the heat source was increased 1.7 kW to 2.8 kW over the time period from 9:39 to 10:09. In each experiment the first flames occurred approximately when the increased electrical power to the strip heaters reached 2.8 kW. The measured CO concentration at the 30.0 m and 45.2 m stations tracked each other closely for all five experiments. These stations are approximately 12 and 19 hydraulic diameters downwind from the source fire. The implication is that, beyond 10 hydraulic diameters, the source fire product emissions are well mixed over the entry cross section.

Table 1. Mine fire experimental conditions.

Experiment number	Volumetric air flow Q, m^3/s	Average air velocity, m/s	Fire source location
1	9.34	1.71	Floor
2	2.74	0.50	Floor
3	6.19	1.13	Floor
4	11.5	2.10	Mid-height
5	5.84	1.07	Mid-height

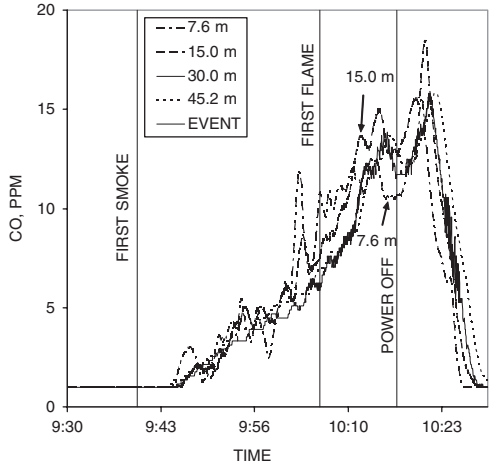

Figure 1. CO concentration at sensor stations in response to coal fire on entry floor for experiment no. 2 at 7.6, 15.0, 30.0, and 45.2 m distance from fire.

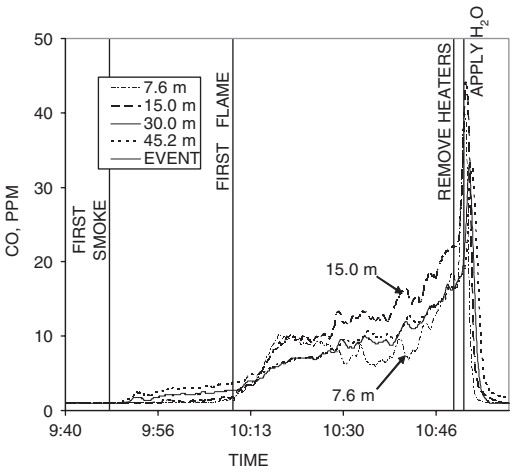

Figure 2. CO concentration at sensor stations in response to coal fire at entry mid-height for experiment no. 5 at 7.6, 15.0, 30.0, and 45.2 m distance from fire.

The CO concentrations at the 7.6 m and 15.0 m stations, which were three and six hydraulic diameters downwind from the fire, had more divergent CO concentrations than those at the 30.0 and 45.2 m stations. The instability of the CO production due to fluctuations in the fire intensity was not averaged out by the air flow in the 15 m zone immediately downwind from the fire. This was observed for all five experiments. In each experiment an approximately linear increase in CO concentration occurred in the smoldering stage, with an increased rate in the flaming stage. For experiment no. 1 there was an electrical power disruption after initial flaming combustion. This resulted in a cooling of the coal and the extinguishment of an early flaming combustion. Power was reapplied, and steady flaming combustion followed.

3.1 *CO alert and alarm*

For each experiment the 5 ppm CO alert value was attained at each of the four sensor stations. Only for experiment no. 2 did the CO alert occur in the smoldering combustion stage. This was a consequence of the lowest volumetric flow rate of 2.74 m^3/s for experiment no. 2. To assure early fire detection in the smoldering stage for volumetric air flow rates greater than 2.74 m^3/s for these small coal fires, either the CO alert values could be lowered or the sensor spacing could be decreased. Reference to volumetric air flow rate must be understood with caution. The air velocity can affect the fire production rate of CO. In addition, the turbulent mixing of the fire POC plume will be affected by the confinement height of the tunnel. However, for early detection of small fires, these effects should be relatively small.

Table 2. Measured values of maximum CO, and CO and smoke optical density, OD, 15 min after flaming combustion 45.2 m downwind from the fire source.

Exp. No.	MAX. CO, ppm	H_R kW,	CO*, ppm	OD*, m^{-1}	H_R^*, kW
1	6.8	17	6.84	—	17
2	15.8	11	14.06	—	10
3	7.8	13	6.64	0.024	11
4	7.2	22	2.54	0.0072	8
5	18	28	7.03	0.022	11

* 15 min after visible flames

At the 7.6 m and 15.0 m stations the 10 ppm CO alarm value occurred for all five experiments. The CO 10 ppm alarm value was not achieved at the 30.0 m and 45.2 m stations for experiment nos. 1, 3, and 4. These latter experiments are associated with the air quantity greater than 6.19 m^3/s, and consequently, CO is subjected to much greater dilution.

3.2 *Fire heat production*

The heat release for coal combustion can be estimated from the CO generated in the flaming combustion mode. The CO generated by the flaming combustion of coal is 4.8 mg/kJ (Egan, 1990). Formally, the heat release H_R (kW) is determined from

$$H_R = 1.25 \times 10^{-6} \times Q \times [CO] / 4.8 \times 10^{-6}, \quad (1)$$

where [CO] is the CO concentration in ppm, and Q is the volumetric air flow in m^3/s.

Since eq (1) depends upon the volumetric air flow, more complete mixing in a mine entry results in a better estimate of the heat production rate when a CO sensor near the roof is used to detect a concentration representative for the cross-section. The observation that the measured CO concentration at the 30.0 m and 45.2 m stations tracked each other provides the CO concentration at the 45.2 m station as an estimate of the heat production rate based upon uniform POC mixing. The maximum CO concentration 45.2 m downwind from the fire is used to represent the maximum heat release rate in the flaming stage. The CO maximum concentration and the associated heat release rate are shown in Table 2. For experiment nos. 1–3 with the fire source on the entry floor the highest maximum CO concentration is associated with the lowest ventilation of experiment no. 2. The maximum CO concentration at the 45.2 m station occurred after the onset of flaming combustion for each experiment. For experiment nos. 1–2 the time at which the maximum CO occurred at the 45.2 m station was approximately 15 min after flaming combustion. The maximum CO at the 45.2 m station occurred at least 30 min after flaming combustion for experiment nos. 3–5. As shown in Table 2

the maximum fire intensities were less than 30 kW for the fire sources used in these experiments. These fire intensities are indicative of a small fire source.

3.3 *CO and smoke 15 min after flaming combustion*

Previous research (Litton, et al., 1991) established the significance for fire detection within 15 min of flaming combustion based upon ignition of a belt fire by a small flaming coal fire. For these experiments, the measured CO concentration 45.2 m downwind from the source fire where the fire POC are well mixed is listed in Table 2 at 15 minutes after flaming combustion. Only for experiment no. 2 with a volumetric air flow of 2.74 m^3/s was the CO concentration greater than the 10 ppm alarm level 15 minutes after flaming combustion. In experiment no. 5, the other experiment in which a CO alarm was reached, the CO did not reach alarm level until 24 min after flaming combustion.

In proximity to the fire, at the 7.6 m station, where the contaminants are less diluted, the CO alarm value was reached for experiment nos. 1 and 5 within 15 min after flaming combustion. For experiment no. 2 the CO alarm value occurred within the smoldering combustion stage. For experiment nos. 3 and 4 the CO alarms did not occur until 34 and 65 min after flaming combustion. This inconsistency of the CO alarm time with air flow further supports the need to lower the CO alarm level or place the sensor closer to any in-mine locations identified as high risk for a potential fire source.

A light obscuration monitor was located 1.6 m upwind from the 45.2 m CO sensor location for experiment nos. 3–5. The light obscuration monitor consisted of an incandescent light source and a photovoltaic cell separated by one meter. The measured light transmission through the light monitor was used to determine the smoke optical density. Table 2 shows for experiment nos. 3 and 5 that 15 minutes after visible flames the CO concentration was in excess of the 5 ppm alert value and the smoke optical density value was greater than the smoke sensor optical density alarm value of 0.022 m^{-1}. The higher ventilation in experiment no. 4 resulted in CO alert and smoke alarm values occurring 65 min and 51 min after visible flames. For this latter case the greater POC dilution suggests that a lower CO or smoke sensor alarm value should be used for earlier fire detection, or the placement of the smoke sensor should be closer to any location identified as high risk for a fire source.

Figure 3 shows the CO concentration 15 min after flaming combustion at the four sensor locations for the five cases. The separation in CO concentration values is more significantly dependent upon ventilation velocity than whether the fire source is on the floor or at mid-height. The lowest CO concentration is associated with the highest air flow of 2.1 m/s. The highest

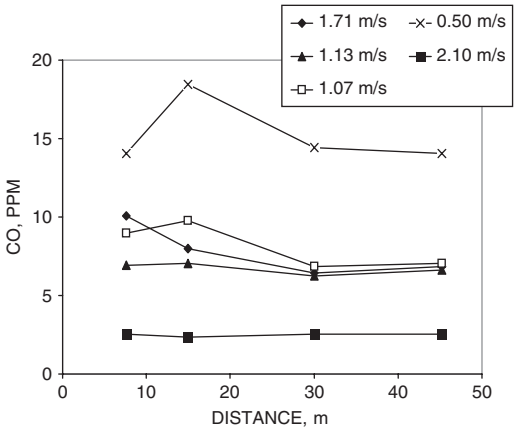

Figure 3. CO concentration 15 min after flaming combustion dependence upon sensor location for average air flows of 0.50, 1.07, 1.13, 1.71, and 2.10 m/s.

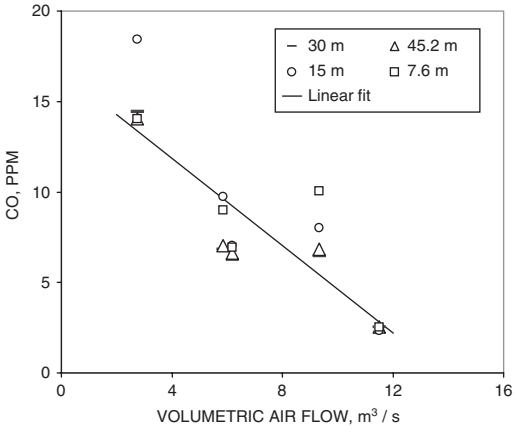

Figure 4. CO concentration 15 min after flaming combustion at 7.6, 15.0, 30.0, and 45.2 m distance from fire.

CO concentrations are associated with the lowest air flow of 0.5 m/s. The intermediate CO concentrations are associated with the range of air flows from 1.07 m/s to 1.71 m/s. There is not a significant variation in the CO concentration between the 30.0 and 45.2 m sensor stations for a specific air flow. Because of the small fire intensities, the air flow has little effect upon the CO production.

Figure 4 shows the dependency of CO concentration upon the volumetric air flow for all four sensor stations 15 min after flaming combustion for all five air flow conditions. The best fit of a linear relationship to the data with an R square value of 0.73 shows that the CO concentration is dependent upon the volumetric air flow, but there is a wide degree of uncertainty. For fires of nearly equal intensity a linear

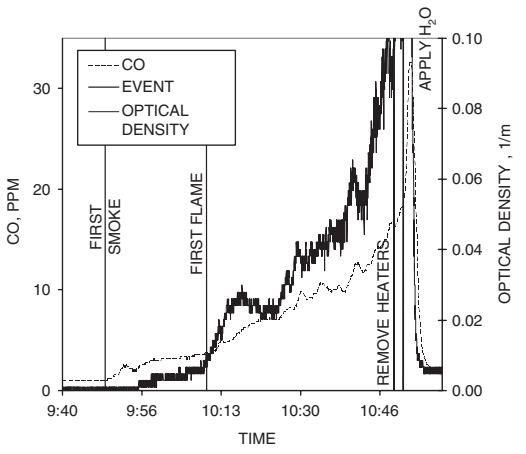

Figure 5. Comparison of CO and smoke optical density at 45.2 m for experiment no. 5.

dependence of CO concentration upon volumetric flow rate is expected. Extrapolation of the linear fit of the data to non-detectable, near zero, CO concentration occurs at a volumetric flow rate of 14 m^3/s. For the 2.08 m by 2.90 m airway considered, the linear air flow rate is 2.32 m/s. These results show the need to set lower CO alarm values for higher air flow conditions in a mine.

3.4 *Correlation of CO and smoke*

Figure 5 shows a comparison of the CO concentration and the smoke optical density at the 45.2 m station for experiment no. 5. The smoke optical density and CO exhibit similar trends over the course of the experiment. An analysis of the optical density D as it is correlated with the CO concentration at the 45.2 m station determined the linear correlation over the combined smoldering and flaming combustion range of the coal fire

$$D = A\,[CO]\,, \tag{2}$$

where A is a proportionality constant.

The values for A and the coefficient of determination R^2 are listed in Table 3 for experiment nos. 3–5. The R square value is not less than 0.79 for these experiments.

The optical density D, measured in units of inverse meters, m^{-1}, is related to the smoke mass concentration C_m by the relationship (Mullholland, 1988)

$$D = (K_m / 2.3)\ C_m, \tag{3}$$

where the specific extinction coefficient K_m depends upon the size distribution and optical properties of the smoke. A combination of equations (2) and (3) yields

$$C_m = (2.3 / K_m)\ A\,[CO] \tag{4}$$

Table 3. Proportionality constant for optical density dependence upon CO concentration.

Experiment number	A	R^2
3	0.0036	0.87
4	0.004	0.79
5	0.0045	0.86

Equation (4) provides an interpretation of the smoke concentration as linearly dependent upon the CO concentration. The fit of the smoke optical density with CO concentration did not distinguish between smoldering and flaming combustion.

The value for A can be selected to be the average of the three values for experiments 3–5. The average value of A is 0.004. This value in equation (2) implies that a 5 ppm CO concentration is associated with an optical density equal to 0.02 m^{-1}, and a 10 ppm CO concentration is associated with an optical density equal to 0.04 m^{-1}. The smoke sensor optical density alarm value of 0.022 m^{-1} would be associated with the 5 ppm CO alert value.

An estimate can be made of K_m based upon its definition in terms of the extinction coefficient Q_e, the smoke particulate mass density ρ, and smoke particulate average diameter d.

$$K_m = 1.5\ Q_e / (\rho\ d) \tag{5}$$

For smoke particulate density 1,400 kg/m^3, diameter of 0.3 micron, and extinction coefficient of 2.5, the value of the specific extinction coefficient is 8,900 m^2/kg. The specific extinction coefficient is comparable to the value of 7,600 m^2/kg (Seader & Einhorn, 1976) for flaming combustion of wood and plastics. The relationship between C_m and [CO] is approximately

$$C_m = 1.03\ X\ 10^{-6}\ [CO]. \tag{6}$$

3.5 *Simulation of CO concentration using FDS*

CO concentrations from the small coal fires were simulated using the Fire Dynamics Simulator (FDS), an existing computational fluid dynamics program (McGrattan, et al., 2002). The chemical structure of the Pittsburgh coal is simplified as $CH_{0.74}O_{0.08}$. CO is assumed to be created with constant yield at the flame and transported with the combustion products. The fraction of fuel mass converted into carbon monoxide is 0.078 obtained for Pittsburgh coal (Egan, 1990). Other important parameters for the CO simulation are the amount of energy released per unit mass of oxygen consumed and the fire heat release rate. The amount of energy released per unit mass of oxygen consumed for

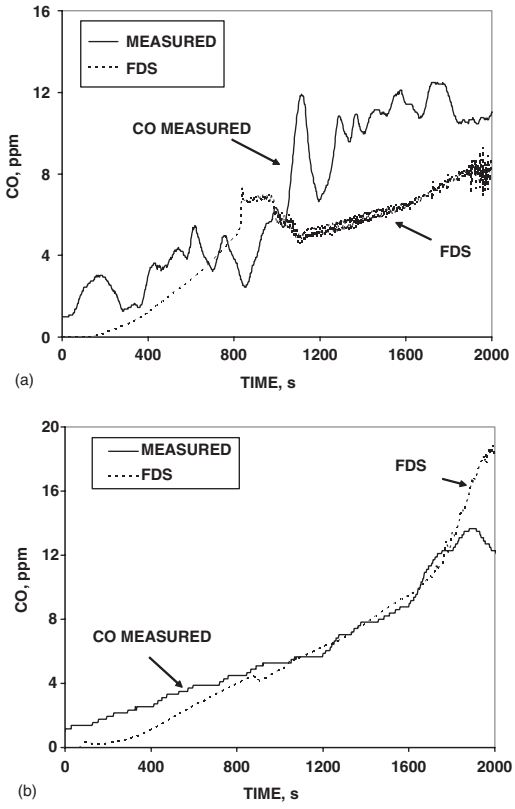

Figure 6. CO concentrations predicted by FDS for experiment no. 2 with fire source on floor (a) at 7.6 m station; (b) at 45.2 m station.

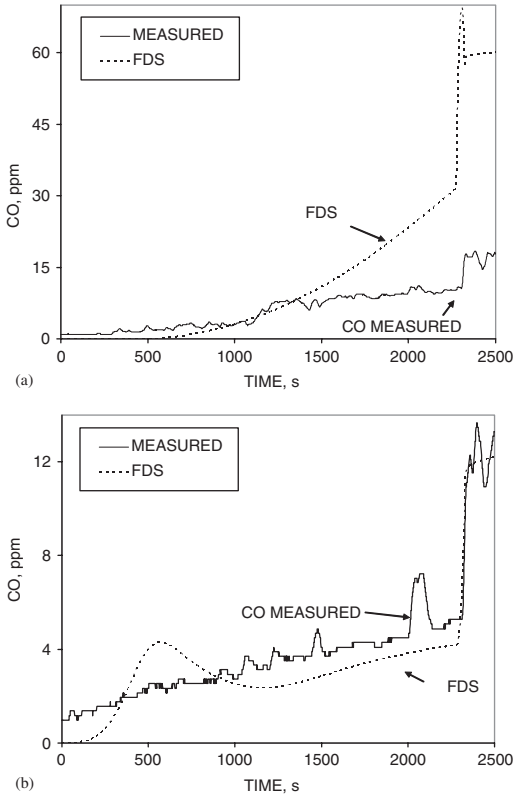

Figure 7. CO concentrations predicted by FDS for experiment no. 4 with fire source at mid-height (a) at 7.6 m station; (b) at 45.2 m station.

Pittsburgh coal is 11,900 kJ/kg derived from the heat of combustion for the coal. From the CO measurements in the experiment, it was determined that the whole coal combustion process can be approximately divided into three stages: the smoldering combustion stage, the flaming combustion stage, and the peak combustion stage. The heat release rates at these three stages increased nearly linearly with the time. For the simulations the heat release rate in each stage was simplified as a linear increase with time. The heat release rates at the end of each stage were estimated by equation (1) with the CO concentration measured at 45.2 m station. For the purpose of early CO alert and alarm, the peak combustion stage may be not important but can be used for the comparison between the simulation and the experiment.

Figures 6 and 7 show the CO concentrations predicted by the FDS for experiments nos. 2 and 4, respectively. For experiment no. 2 with the fire source at the floor, FDS prediction was in good agreement with the experiment at 45.2 m station while the FDS predicted lower CO concentration than the experiment after 1,000 s at 7.6 m station. This is probably because the fraction of fuel mass converted into carbon monoxide was not always constant in the experiment. For experiment no. 4 with the fire source at the mid-height, FDS prediction was much higher than the experiment after 1,500 s at 7.6 m station while a peak occurred in FDS simulation before 1,000 s at 45.2 m station. Generally speaking, FDS simulation agrees well for the experiment with the fire source at the floor and can be used to optimize the CO sensor spacing. Further modeling work is needed to improve the simulation with the fire source at the mid-height.

4 CONCLUSIONS

For the small, less than 30 kW heat release rate intensity, coal fires in a 2.08 m high and 2.90 m wide entry, it was determined that:

- At distances greater than 10 hydraulic diameters from the source fire, the CO concentration was well-mixed over the entry.

- To assure detection in the coal fire smoldering stage, it would be beneficial to decrease the alert and alarm CO concentration values for volumetric air flows greater then 2.74 m^3/s.
- Relatively close to the potential fire source, within 15 m of the fire, CO 10 ppm alarm values occurred for the volumetric air flows less than 11.5 m^3/s. For air quantities greater than 6.19 m^3/s, the 10 ppm CO alarm did not occur at distances greater then 30.0 m downwind from the fire. This is consistent with the requirement of the Code of Federal Regulations (2004) that any CO sensor be less than 30.5 m (100 ft) downwind from each belt drive unit.
- For volumetric air flow rates greater than 2.74 m^3/s, a CO alarm was not achieved within 15 min after the onset of flaming combustion 45.2 m distance from the source fire. At a distance of 7.6 m from the fire the occurrence of a CO alarm value was not consistent with the air flows. This suggests the use of lower CO alarm values for a CO sensor downwind from a potential fire source, such as a belt drive.
- Extrapolation of CO concentration 15 min after flaming combustion with air flow showed that the CO concentration would not be detectable for air flows greater than of 2.32 m/s at distances greater than 7.6 m from the source fire.
- CO concentration correlates with smoke mass concentration and optical density.
- FDS simulation agreed well for the experiment with the fire source at the floor and can be used to optimize the CO sensor spacing. Further modeling work is needed to improve the simulation with the fire source at the mid-height.

REFERENCES

Code of Federal Regulations. 2004. 30 CFR, Part 75.351 (e). Office of the Federal Register, National Archives and Standards Administration, U.S. Government Printing office, Washington, D.C.

Egan, M.R. 1990. Summary of combustion products from mine materials: their relevance to mine fire detection. *U.S. Bureau of Mines Informational Circular 9272*, 12 pages.

Litton, C.D., Lazzara, C.P., & Perzak, F.J. 1991. Fire detection for conveyor belt entries. *U.S. Bureau of Mines RI 9380,* 21 pages.

McGrattan, K.B., Forney, G.P., Floyd, J.E., Hostikka, S., & Prasad, K. 2002. Fire Dynamics Simulator (Version 3) User's Guide, U.S. Dept. of Commerce. National Institute of Standards and Technology.

Mullholland, G.W. 1988. Smoke production and properties. The SFPE Handbook of Fire Protection Engineering. Section 1/Ch. 25, (Ed.-in-chief, P.H. DiNenno, National Fire Protection Association, Quincy, MA).

Seader, J.D., & Einhorn, I.N. 1976. Some physical, chemical, toxological and physiological aspects of fire smokes. *16th Symp. (Int.) on Combustion, MIT, Cambridge, MA. August 15–20, 1976*, (The Combustion Institute, Pittsburgh, PA), pp.1423–1445.